Journal of Membrane Science 326 (2009) 316–321

Contents lists available at ScienceDirect

Journal of Membrane Science

journal homepage: www.elsevier.com/locate/memsci

Cobalt-doped silica membranes for gas separation

David Uhlmann[a], Shaomin Liu[a], Bradley P. Ladewig[b], João C. Diniz da Costa[a,*]

[a] FIMLab – Films and Inorganic Membrane Laboratory, Division of Chemical Engineering, The University of Queensland, Brisbane, QLD 4072, Australia
[b] ARC Centre of Excellence for Functional Nanomaterials, Australian Institute of Bioengineering and Nanotechnology, The University of Queensland, Brisbane, QLD 4072, Australia

ARTICLE INFO

Article history:
Received 13 June 2008
Received in revised form 26 August 2008
Accepted 6 October 2008
Available online 19 October 2008

Keywords:
Cobalt
Silica
Hydro-stability
Selectivity
Gas separation

ABSTRACT

Cobalt-doped silica membranes were synthesized using tetraethyl orthosilicate-derived sol mixed with cobalt nitrate hexahydrate. The cobalt-doped silica structural characterization showed the formation of crystalline Co_3O_4 and silanol groups upon calcination. The metal oxide phase was sequentially reduced at high temperature in rich hydrogen atmosphere resulting in the production of high quality membranes. The cobalt concentration was almost constant throughout the film depth, though the silica to cobalt ratio changed from 33:1 at the surface to 7:1 at the interface with the alumina layer. It is possible that cobalt has more affinity to alumina, thus forming $CoOAl_2O_3$. The He/N_2 selectivities reached 350 and 570 at 160 °C for dry and 100 °C wet gas testing, respectively. Subsequent exposure to water vapour, the membranes was regenerated under dry gas condition and He/N_2 selectivities significantly improved to 1100. The permeation of gases generally followed a temperature dependency flux or activated transport, with best helium permeation and activation energy results of 9.5×10^{-8} mol m^{-2} s^{-1} Pa^{-1} and 15 kJ mol^{-1}. Exposure of the membranes to water vapour led to a reduction in the permeation of nitrogen, attributed to water adsorption and structural changes of the silica matrix. However, the overall integrity of the cobalt-doped silica membrane was retained, given an indication that cobalt was able to counteract to some extent the effect of water on the silica matrix. These results show the potential for metal doping to create membranes suited for industrial gas separation.

1. Introduction

Inorganic membranes have attracted great interest for gas separation applications in industries such as coal gasification [1,2], steam methane reforming [3], water–gas shift reaction [4] and fuel cell systems [5,6]. Typically these industries may require gas separation at temperatures preferably between 100 and 500 °C, which can be met by the employment of silica or metal-based membranes. Ultra microporous silica membranes are generally easy to synthesize by sol–gel or chemical vapour deposition (CVD) methods and cheap to produce. It is a general trend in the literature that there is often a trade-off between permeability and selectivity in both types of membranes, as sol–gel membranes deliver higher fluxes while CVD membranes higher selectivities.

One of the major concerns with silica-derived membranes relate to their structural integrity and stability for wet gas stream exposure which is generally the case in industrial gas processing. The morphology of silica has been shown to alter upon exposure to steam [7–9], mainly directly attributed to the collapse of small pores and expansion of larger pores, resulting in a loss of selectivity [10]. To address this problem, some research groups [6,11–13] incorporated templates into the silica film whereby the membrane films were calcined in non-oxidizing atmospheres. As a result, templated silica membranes imparted hydrostable properties, accompanied by structural modifications. For instance, gas selectivity was lowered as covalent ligand methyl template in methyltriethoxysilane led to the formation of slightly larger pore sizes [11]. On the other hand, Duke et al. [6] reported improved gas selectivity by exposing to steam silica membranes with carbonized templates derived from C6 surfactant triethylhexylammonium bromide (C6HAB).

Departing from techniques to reduce the hydrophilicity of silica, some research groups have doped metals into silica matrices to reduce the degradation of a hydrophilic membrane. Fotou et al. [14] experimented with doping of alumina and magnesia by mixing pure silica sols with ethanol solutions of the metal salts. Alumina doping of 3% and 6% did not change the silica structure and gave enhanced stability against hydrothermal treatment. The magnesia doping of 3% appeared to significantly reduce the silica surface area and not provide enhanced stability. Gu et al. [15] achieved enhanced hydrothermal stability using 3% alumina doping in CVD

* Corresponding author. Tel.: +61 7 3365 6960; fax: +61 7 3365 4199.
E-mail address: j.dacosta@uq.edu.au (J.C. Diniz da Costa).

0376-7388/$ – see front matter © 2008 Elsevier B.V. All rights reserved.
doi:10.1016/j.memsci.2008.10.015

membranes reporting a stable 45% hydrogen permeance reduction after long-term exposure to steam. Kanezashi and Asaeda [16] found the incorporation of 33% nickel doping to improve hydrothermal stability. Both hydrogen and nitrogen permeance decreased by 60% and 93%, respectively upon exposure to high temperature water vapour, favouring high H_2/N_2 selectivity.

Very recently, a limited number of research works has been published on high quality metal-doped silica membranes. This includes doping the silica matrix with nickel [16–18] and cobalt [19,20]. In all cases the metal oxide in the silica matrices of the membranes were chemically reduced to pure metal by a flow of hydrogen at elevated temperature. The characterization of metal-doped silica membranes and xerogels reported in the literature is also limited. X-ray diffraction (XRD) analysis by Kanezashi et al. [17] showed that nickel-doped silica resulted in strong NiO peaks upon calcination at 500 °C. Ikuhara et al. [18] further showed that NiO phase changed to pure Ni upon reduction in a H_2 atmosphere. Similarly, cobalt-doped silica resulted in the formation of Co_3O_4 peaks upon calcination at 400–600 °C [21] and the reduction to CoO and Co under calcinations in H_2 atmosphere at 600 °C [20].

In this work, we report the development of cobalt-doped silica membranes reaching He/N_2 selectivities as high as 350 and 1100 for dry gas and after water vapour exposure, respectively. Gas permeation tests were carried out for helium and nitrogen at temperatures between 25 and 190 °C. The membranes were characterized using X-ray photoelectron spectroscopy (XPS) and scanning electron microscopy (SEM) to detect the thickness of the layer and the sharpness of the transition between layers. The cobalt-doped silica xerogel structural properties were studied using fourier transform infrared (FTIR) and XRD to determine functional groups and phases, and gravimetric adsorption to determine water adsorption.

2. Experimental

2.1. Sol–gel and xerogel preparation

Experimental sol–gel solutions were prepared from tetraethylorthosilane (TEOS), absolute ethanol (EtOH), 30% hydrogen peroxide (H_2O_2) in water (H_2O) and cobalt nitrate hexahydrate ($Co(NO_3)_2{\cdot}6H_2O$); a molar ratio of 255 EtOH:4 TEOS:1 $Co(NO_3)_2{\cdot}6H_2O$:9 H_2O_2:40 H_2O. Similarly, a blank silica sol–gel solution for comparison purposes only was prepared using the same procedure described but replacing cobalt nitrate hexahydrate with nitric acid and water, in such a way to effectively replace each Co^{2+} ion with $2H^+$ ions. The final molar ratio of this solution was 255 EtOH:4 TEOS:2 HNO_3:9 H_2O_2:46 H_2O. An aliquot of each sol sample was dried in a temperature-controlled oven at 60 °C in ambient pressure air to form a xerogel. The xerogel samples were crushed finely and calcined with ramp rates of 2 °C min^{-1} to 600 °C in ambient pressure air and held for 4 h. After characterization experiments were performed, the calcined cobalt-doped silica xerogel samples were subsequently reduced in a rich hydrogen atmosphere at 500 °C for 15 h for further analysis.

2.2. Characterization

Fourier transform infrared characterization was carried out to determine functional groups within the bulk silica matrix using a Nicolet 6700 FT-IR, with range of 30,000–200 cm^{-1}. XRD for phase detection was conducted using a Bruker D8 Advance with a graphite monochromator using Cu Kα radiation. The tested range of 2θ was from 15° to 70°. Gravimetric water adsorption measurements were performed with an in-house adsorption apparatus with quartz springs, a MKS pressure transducer and a temperature-controlled oven. Xerogel samples were degassed overnight at $P < 0.2$ Pa at 300 °C prior to water adsorption experiments. The 3% water adsorption was calculated from the water adsorption isotherms.

Scanning electron microscopy was performed using a JEOL JSM-6400F scanning electron microscope. Membrane cross-sections were made conductive using platinum coating with an EIKO coating apparatus in high purity argon. XPS auger microscopy was performed using a KRATOS Axis Ultra and depth profiling was performed using a differentially pumped Kratos Minibeam III ion gun using 4 keV argon ions at an ion source extractor current of 630 nA. The order of sputter rates for silicon was in the region of 60 nm h^{-1} and the sputtered area formed a rhombus of 9 mm × 9 mm. The analyzed surface was centred in the rhombus with a diameter of 4 mm. This allowed for a complimentary method of measuring the membrane thickness and analysis of the cobalt-doped silica to alumina interface through a depth profile.

2.3. Membrane preparation

Commercial alumina platelet substrates (Rojan Ceramics, Australia), with porosity of 30% and an average pore size of 0.5–1 μm were coated with 3 layers of an alumina-based solution made of Locron (Clariant, Germany) and 0.0007 M $HNO_3{}^-{}_{(aq)}$ prepared in a 4:1 ratio refluxed at 80 °C for 16 h. The dip-coating used a controlled immersion time of 1 min, and immersion/withdrawal speed of 2 cm min^{-1}. Subsequent calcinations of each layer were carried out at 600 °C in ambient pressure air, and held for 4 h with a heating and cooling rate of 1 °C min^{-1}. A total of 6 layers of cobalt-doped silica sol–gel solution were coated onto the alumina layers in similar fashion but using a heating and cooling rate of 0.7 °C min^{-1}. After calcination of the last cobalt-doped silica layer, the membrane was exposed to a pure hydrogen atmosphere at 500 °C for 15 h to reduce cobalt oxides in the silica matrix followed by 0.7 °C min^{-1} cooling rate.

2.4. Gas permeation testing

Single permeation tests were conducted in a custom-made permeation setup (Fig. 1) with a membrane housing module. The temperature of the module was controlled by a heating element with an external PID temperature controller. The gas feed stream

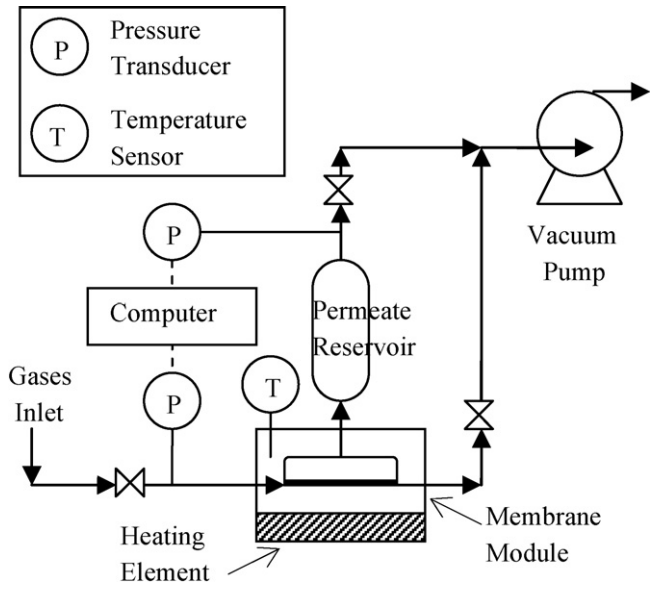

Fig. 1. Permeation setup.

was connected to an MKS pressure transducer and four gas inlets, with the appropriate gas selected by valves. The permeate stream of the module was connected to a permeate reservoir and a second MKS pressure transducer. Both sides of the membrane were also connected to a rotary vacuum pump, to allow evacuation of the permeate line between each test, and evacuation of the retentate line when changing gases. Both pressure transducers were connected to a computer for data logging.

Tests were carried out by controlling the pressure of the feed stream to a desired value, and evacuating the permeate side to a vacuum pressure. The permeate stream valve was then closed allowing pressure to build in the permeate reservoir due to gas permeation though the membrane. The collected data was used to calculate the permeance according to Eq. (1), where P_f is the pressure of the feed line (Pa), $P_{p,0}$ is the initial pressure at ~0.2 Pa at the permeate line (Pa), $P_{p(t)}$ is the transient pressure measured in the permeate volume (Pa), V_p (m^3) is the constant permeate reservoir volume, A is the permeable membrane area (m^2), R is the ideal gas constant (kJ $kmol^{-1}$ K^{-1}), and T is temperature (K). Permeation experiments were carried out for helium and nitrogen within a membrane temperature range of 20–190 °C due to the limitations imposed by seals.

$$\text{Permeance} = \frac{d}{dt}\left(\ln\left(\frac{P_f - P_{p,0}}{P_f - P_{p(t)}}\right)\right) \cdot \frac{V_p}{A \cdot R \cdot T} \quad (1)$$

Subsequently to dry gas stream tests, the membranes were exposed to water vapour for 5 h at 180 °C by passing an ambient temperature gas stream through a water bubbler, resulting in 3 vol% water concentration. The membranes were subsequently tested for 3 vol% wet gas streams for temperatures ranging from 50 to 180 °C. Upon completion of these tests, the membranes were regenerated by exposing the membranes to dry helium gas streams for 5 h at 190 °C. The regenerated membranes were tested as described above from 50 to 190 °C.

3. Results

Fig. 2 compares the FTIR spectra of the blank silica, cobalt-doped silica, and reduced cobalt-doped silica xerogel samples calcined at 600 °C. Bands at 460, 800 and 1080 cm^{-1} were assigned to siloxane bonds (Si—O—Si), at 950 cm^{-1} to silanol bonds (Si—O—H) [22]. The IR bands allocated to Co_3O_4 appeared at 570 and 670 cm^{-1} [23,24]. Reduction of Co_3O_4 in the cobalt-doped sample was observed after hydrogen treatment, as the Co_3O_4 peaks were no longer present. No intermediate CoO peaks were distinguishable at 590, 720, and 1450 cm^{-1} [25]. The blank silica differed significantly from the cobalt-doped silica samples, forming mostly IR bands assigned to Si—O—Si bonds.

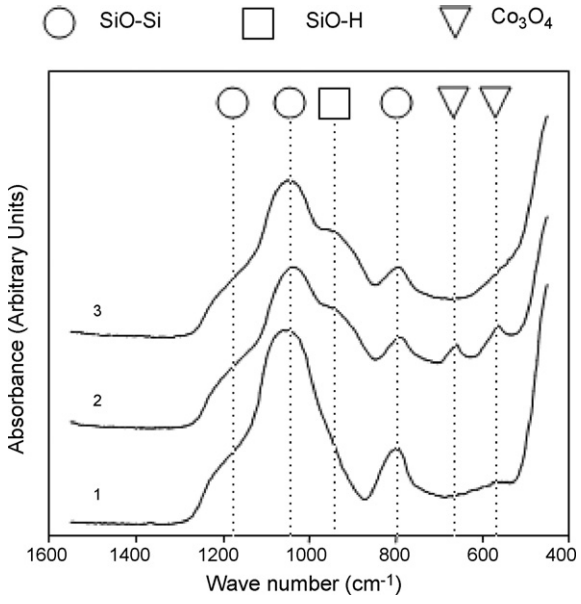

Fig. 2. FTIR spectra of xerogels calcined at 600 °C in air (1) pure silica, (2) cobalt-doped silica and (3) reduced cobalt-doped silica.

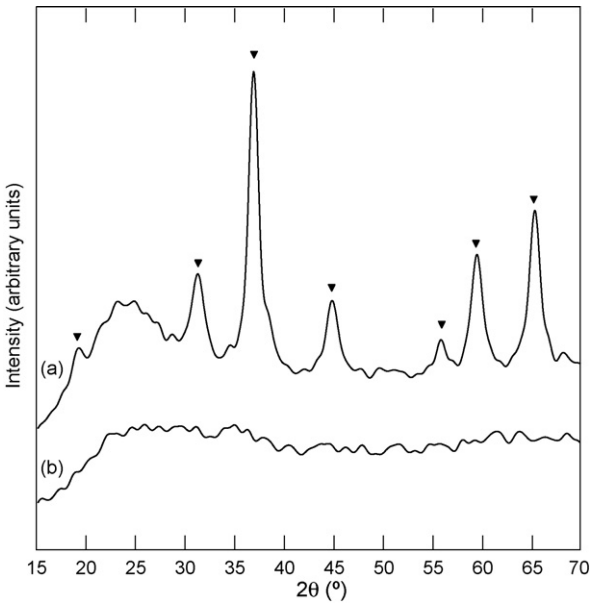

Fig. 3. XRD spectra of (a) cobalt-doped silica and (b) reduced cobalt-doped silica, where (▼) Co_3O_4.

The X-ray diffraction spectra of xerogel samples are shown in Fig. 3. The silica xerogel samples were amorphous and characterized by broad humps and the cobalt-doped xerogel calcined in air clearly displayed a crystalline phase of Co_3O_4. Confirming the IR analysis, upon hydrogen reduction the cobalt-doped xerogel lost its crystalline structure, showing no Co_3O_4 or CoO peaks, only broad humps similar to amorphous silica.

Fig. 4 shows the XPS sputter profile for the relative concentration of oxygen, aluminium, silicon and cobalt as a function of the top layer depth of the membrane surface. The results showed a decrease of silica concentration connected with an increase of alumina beginning from a depth of 70 nm. The interface between the silica film and alumina substrate crossed over at approximately 330 nm. Cobalt concentration was fairly constant throughout the profile and was expected to exist throughout the depth of the silica layer. SEM of the membrane cross-section showed the porous coarse α-Al_2O_3 substrate pictured on the right of Fig. 5. Locron was used as a primer layer to form γ-alumina, reducing the roughness of the substrate. The cobalt-doped silica layer is distinctive at the far left, though the SEM micrograph does not clearly distinguish the top layer from the intermediate γ-alumina or substrate α-Al_2O_3 layer.

The water adsorption results for 3 vol% water vapour exposure are listed in Table 1. The cobalt-doped silica and the silica xerogels were hydrophilic as both samples adsorbed water. However, the cobalt-doped silica xerogel had a lower water adsorption capacity than the pure silica xerogel. The permeation of gases for dry, wet, and regenerated dry (R-Dry) streams as a function of temperature for the cobalt-doped silica membranes are shown in Fig. 6. The permeance of helium increased with temperature for all tests while

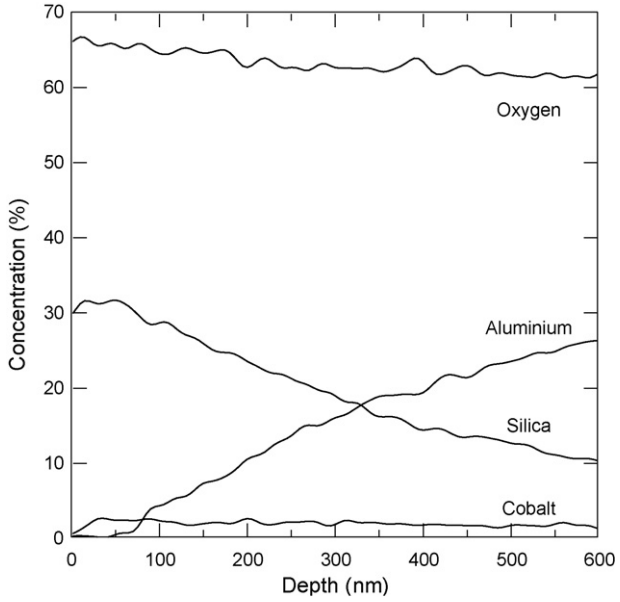

Fig. 4. XPS sputter profile of cobalt-doped silica membrane.

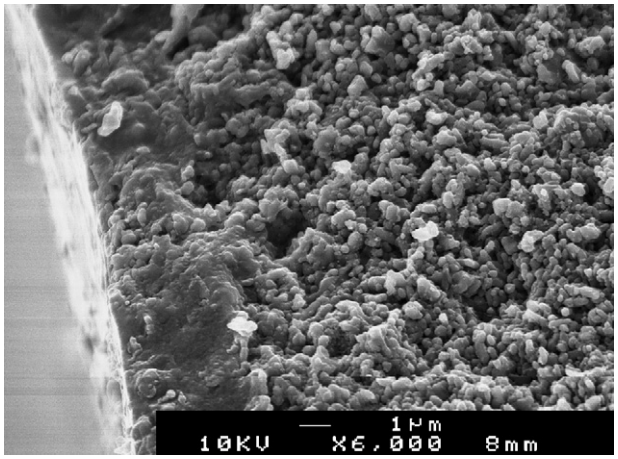

Fig. 5. SEM image of cobalt-doped silica membrane.

nitrogen showed the opposite effect, except for temperatures above 100 °C for wet gas stream tests. These results are consistent with activated transport or molecular sieving mechanism as reported in the literature [6,26,27], thus following a temperature dependency flux as shown in Eq. (2):

$$J_x = -D_O K_O \exp\left(\frac{-E_{act}}{RT}\right)\frac{dp}{dx} \quad (2)$$

where J is the flux (mol m^{-2} s^{-1}) through the membrane, E_{act} (kJ mol^{-1}) is an apparent activation energy, R the gas constant (kJ mol^{-1} K^{-1}) and T the absolute temperature (K), D_o and K_o are temperature independent proportionalities for the Arrhenius

Table 1
Water adsorption on cobalt-doped silica xerogel.

Temperature (°C)	Water adsorption mmol g^{-1}	
	Silica xerogel	Cobalt-doped silica xerogel
30	8.34	4.87
60	3.53	1.14
100	1.25	0.55

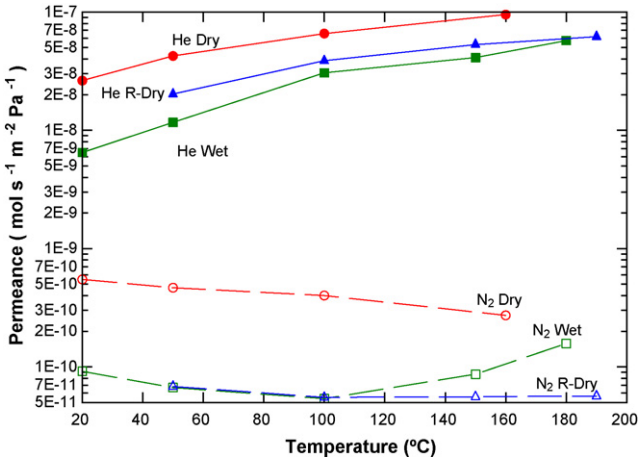

Fig. 6. Permeance (±6%) of gases through cobalt-doped silica membrane.

Table 2
Activation energies of gases through the membrane.

	Activation energy of helium (kJ mol^{-1})	Activation energy of nitrogen (kJ mol^{-1})
Dry	9.5	−5.0
Wet	15.0	[a]
R-Dry	10.0	−1.6

[a] Experimental results showed change in activation energy.

and Van't Hoff equations, respectively. This equation has been derived from Barrer [28] proposed model of transport through microporous crystalline membrane. The maximum permeance at 9.5×10^{-8} mol s^{-1} m^{-2} kPa^{-1} was observed at 160 °C for helium at dry gas testing. At the same temperature, nitrogen permeated at 2–3 orders of magnitude lower. The calculated activation energies of the gases through the membrane are given in Table 2, whereas the highest (15.0 kJ mol^{-1}) and lowest values (−5.0 kJ mol^{-1}) were observed for helium and nitrogen at wet gas testing, respectively. The activation energies were calculated based on Arrhenius relation of the natural log of permeance flux over the inverse of temperature.

Wet gas stream containing 3% water vapour affected the permeation of both helium and nitrogen. Under this testing condition, the permeation results generally decreased but still complied with activated diffusion, though a minimum permeation was observed for nitrogen wet gas testing at 100 °C. While the decrease in helium was ~55%, the decrease in nitrogen permeation was ~85%. As a

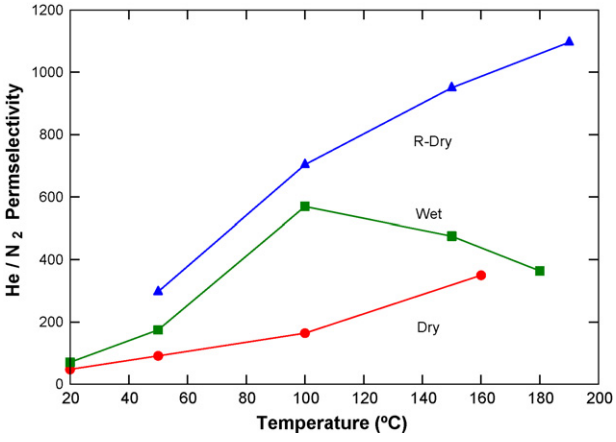

Fig. 7. Selectivity of gases through cobalt-doped silica membrane.

result, Fig. 7 shows that the He/N_2 selectivity at 100 °C increased to 570 as compared to dry gas testing condition, reducing afterwards to levels very close to the latter. Upon regeneration and dry test conditions, the He/N_2 selectivity reached 1100 at 190 °C which is a value generally afforded by CVD membranes (>1000 [29–31]) instead of sol–gel-derived membranes.

4. Discussion

High quality membranes were produced with helium permeation close to 1.0×10^{-7} mol m^{-2} s^{-1} Pa^{-1} and He/N_2 selectivities as high as 1100. These membranes showed great increase in selectivity after exposure to 3% water vapour as He/N_2 selectivity jumped to 570 at 100 °C while a remarkable increase occurred after regeneration and dry gas testing reaching 1100 at 190 °C. The membranes consistently complied with molecular sieving or activated transport mechanism. For every testing condition, the smaller molecule He (d_k = 2.6 Å [32]) resulted in a positive activation energy while the larger molecule N_2 (d_k = 3.64 Å [32]) showed a negative activation energy, except that water has affected the nitrogen permeation during wet gas testing with a minimum permeance occurring at 100 °C. These results indicate that high pore size tailorability was attained, and the average pore sizes were likely to be closer to the kinetic diameter of helium.

This is an unusual and significant finding as after most water vapour treatment experiments in the literature including metal doping, results in higher permeations of the larger gases and therefore a reduction of selectivity. This effect may be explained by the presence of the cobalt phase providing a higher resistance against the structural degradation of the membrane by water vapour attack similar to other metal dopants reported in the literature [14,16,18,19]. Although the silica amorphous phase is hydrophilic and susceptible to reaction and modification by water vapour, the cobalt phase may provide the structural integrity to mostly counteract the effect of water on the silica structure. In turn, this resulted in only a slight collapse of the smaller pores and forming a smaller average pore size with a higher selective, but slightly less permeable membrane. In addition, water was desorbed by regenerating the membrane after exposure to water vapour. This process also allowed for de-blocking of small pores as the kinetic diameter of water is very small (d_k = 2.96 [33,34]). As a result, the permeation of helium increased, but the pore size remained too small for the nitrogen to achieve the same permeation seen before water vapour exposure.

The water adsorption tests revealed that the cobalt-doped silica is hydrophilic, though water adsorption reduced with temperature to very low coverage. For the wet gas stream testing conditions in this work (i.e. 3 vol% water vapour), the uptake of water at low relative pressure ($P/P_0 < 0.2$) corresponded to bonding to surface silanol groups [10]. The FTIR spectra gave a good indication of silanol groups in the cobalt-doped silica xerogel samples. Water vapour interacts strongly with surface silanol because of the water dipole moment and hydrogen bonding property [35]. As nitrogen permeation increased after 100 °C during wet gas testing, this result suggested that the strong water interaction allowed for structural modification in the silica matrix at this point.

From data of both FTIR and XRD spectra it is clear that upon calcination of the cobalt-doped silica, Co_3O_4 was formed, and that after reduction in hydrogen at 500 °C for 15 h no Co_3O_4 or CoO was observed. The cobalt phase was most likely reduced to elemental cobalt. This change of phase, regardless to which phase transpires, may result in a morphological change in the silica xerogel structure. Co_3O_4 may form large structural domains as compared to the silica microstructure due to its crystalline structure. The reduction process may create micro-voids between the cobalt phase and the surrounding film matrix to form structures different from a conventional pure silica matrix. In addition to this, the FTIR spectra also showed that cobalt doping has changed the silica structure for samples calcined at 600 °C, in particular the shoulder assigned to silanol groups at 950 cm^{-1} which was not apparently evident for the blank silica xerogel. These results strongly suggest that the cobalt doping has inhibited the condensation reactions, thus forming a less rigid weakly branched silica matrix.

Although the average membrane thickness was determined to be approximately 330 nm, in fact silica diffused through the alumina particles pores of the intermediate and substrate layer. The SEM micrograph indicated that this was the case, as the top film layer shows continuity through the intermediate layer, prior to the porous α-Al_2O_3 substrate. The silica phase gradually decreased with membrane depth, but the cobalt phase appeared to be consistent throughout the depth of the membrane. Hence, there was a molar ratio disparity resulting from the film deposition procedure and/or film formation. In the sol–gel synthesis process, the silica to cobalt ratio was 4:1. For the final membrane, the molar ratios for the reduced cobalt-doped silica phase changed from 33:1 at the surface, to ~12:1 at 50 nm, ~7:1 at 330 nm and 6:1 at 600 nm. These results may suggest that the cobalt ions in solution have higher affinity to alumina as the initial coatings possibly resulted in the formation of some $CoOAl_2O_3$ phase.

5. Conclusion

High quality cobalt-doped silica membranes were synthesized showing a temperature dependency flux of activated transport. The membranes exposed to water vapour underwent a slight closure of the silica pores, resulting in the reduction of permeation for both helium and nitrogen. When the water vapour was removed after regenerating the membranes, the He/N_2 selectivity increased significantly to 1100 at 190 °C. These results strongly suggest that the membranes pores did not collapse under water vapour exposure, most likely attributed to the extra support provided by the cobalt phase within the silica matrix. XRD and FTIR analysis showed crystalline Co_3O_4 phase present within the membrane which was subsequently reduced at high temperature hydrogen treatment. Although the cobalt concentration was almost constant throughout the membrane film, the silica to cobalt ratio reduced from the membrane surface to the interface with the alumina layer, suggesting that cobalt has more affinity to alumina. The overall doping and reduction technique appeared to form a very different silica xerogel structure than that of a comparable non-doped silica xerogel and displaying a lower water adsorption capacity. Therefore the doping of cobalt into a silica sol–gel influenced the silica membrane structure in a way to provide a hydrostable and highly selective membrane.

References

[1] L. Barelli, G. Bidini, F. Gallorini, S. Servilli, Hydrogen production through sorption-enhanced steam methane reforming and membrane technology: a review, Energy 33 (2008) 554.
[2] M.D. Dolan, N.C. Dave, A.Y. Ilyushechkin, L.D. Morpeth, K.G. McLennan, Composition and operation of hydrogen-selective amorphous alloy membranes, J. Membr. Sci. 285 (2006) 30.
[3] G.Q. Lu, J.C. Diniz da Costa, M. Duke, S. Giessler, R. Socolow, R.H. Wiliams, T. Kreutz, Inorganic membranes for hydrogen produced and purification: a critical review and perspective, J. Colloid Interface Sci. 314 (2007) 589.
[4] G. Barbieri, A. Brunetti, T. Granato, P. Bernardo, E. Drioli, Engineering evaluations of a catalytic membrane reactor for the water gas shift reaction, Ind. Eng. Chem. Res. 44 (2005) 7676.
[5] K. Damen, M. van Troost, A. Faaij, W. Turkenburg, A comparison of electricity and hydrogen production systems with CO_2 capture and storage. Part A: Review and selection of promising conversion and capture technologies, Prog. Energy Combust. Sci. 32 (2006) 215.

[6] M.C. Duke, J.C. Diniz da Costa, G.Q. Lu, M. Petch, P. Gray, Carbonised template molecular sieve silica membranes in fuel processing systems: permeation, hydrostability and regeneration, J. Membr. Sci. 241 (2004) 325.
[7] S. Giessler, L. Jordan, J.C. Diniz da Costa, G.Q. Lu, Performance of hydrophobic and hydrophilic silica membrane reactors for the water gas shift reaction, Sep. Purif. Technol. 32 (1–3) (2003) 255.
[8] I. Imai, H. Morimoto, A. Tominaga, H. Hirashima, Structural changes in sol–gel derived SiO_2 and TiO_2 films by exposure to water vapour, J. Sol–Gel Sci. Technol. 10 (1997) 45.
[9] B.K. Sea, M. Watanabe, K. Kusakabe, S. Morooka, S.S. Kim, Formation of hydrogen permselective silica membrane for elevated temperature hydrogen recovery from a mixture containing steam, Gas Sep. Purif. 10 (3) (1996) 187.
[10] M.C. Duke, J.C. Diniz da Costa, D.D. Do, P.G. Gray, G.Q. Lu, Hydrothermally robust molecular sieve silica for wet gas separation, Adv. Func. Mater. 16 (2006) 1215.
[11] R.M. de Vos, W.F. Maier, H. Verweij, Hydrophobic silica membranes for gas separation, J. Membr. Sci. 158 (1999) 277.
[12] S. Giessler, J.C. Diniz da Costa, G.Q. Lu, Hydrophobicity of templated silica xerogels for molecular sieving applications, J. Nanosci. Nanotechnol. 1 (3) (2001) 331.
[13] C.H. Tsai, S.Y. Tam, Y. Lu, C.J. Brinker, Dual-layer asymmetric microporous silica membranes, J. Membr. Sci. 169 (2000) 255.
[14] G.P. Fotou, Y.S. Lin, S.E. Pratsinis, Hydrothermal stability of pure and modified microporous silica membranes, J. Mater. Sci. 271 (1995) 86.
[15] Y. Gu, P. Harcarlioglu, S.T. Oyama, Hydrothermally stable silica–alumina composite membranes for hydrogen separation, J. Membr. Sci. 310 (2008) 28.
[16] M. Kanezashi, M. Asaeda, Hydrogen permeation characteristics and stability of Ni-doped silica membranes in steam at high temperature, J. Membr. Sci. 271 (2006) 86.
[17] M. Kanezashi, T. Fujita, M. Asaeda, Nickel-doped silica membranes for separation of heluim from organic gas mixtures, Sep. Sci. Technol. 40 (2005) 225.
[18] Y. Ikuhara, H. Mori, T. Saito, Y. Iwamoto, High-temperature hydrogen adsorption properties of precursor-derived nickel nanoparticle-dispersed amorphous silica, J. Am. Ceram. Soc. 90 (2) (2007) 546.
[19] S. Battersby, M.C. Duke, S. Liu, V. Rudolph, J.C. Diniz da Costa, Metal-doped silica membrane reactor: operational effects of reaction and permeation for the water gas shift reaction, J. Membr. Sci. 316 (2008) 46.
[20] H. Mori, T. Nagano, S. Fujisaki, T. Sumino, Y. Iwamoto, Hydrogen permeation through cobalt-doped amorphous silica composite membranes, in: International Conference on Inorganic Membranes, Lillehammer, Norway, 2006.
[21] G. Ortega-Zarzosa, C. Araujo-Andrade, M.E. Compean-Jasso, J.R. Martinez, Cobalt oxide/silica xerogels powders: X-ray diffraction, infrared and visible absorption studies, J. Sol–Gel Sci. Technol. 24 (2002) 23.
[22] Z. Olejniczak, M. Leczka, K. Cholewa-Kowalska, K. Wojtach, M. Rokita, W. Mozgawa, 29Si MAS NMR and FTIR study of inorganic–organic hybrid gels, J. Mol. Struct. 744–747 (2005) 465.
[23] A.Y. Khodakov, J. Lynch, D. Bazin, B. Rebours, N. Zanier, B. Moisson, P. Chaumette, Reducibility of cobalt species in silica-supported Fischer–Tropsch catalysts, J. Catal. 168 (1997) 16.
[24] B. Pejova, A. Isahi, M. Najdoski, I. Grozadanov, Fabrication and characterisation of nanocrystalline cobalt oxide thin films, Mater. Res. Bull. 36 (2001) 161.
[25] R.A. Nyquist, C.L. Putzig, M.A. Leugers, The Handbook of Infrared and Raman Spectra of Inorganic Compounds and Organic Salts, Academic Press, San Diego, 1997.
[26] R.M. de Vos, H. Verweij, Improved performance of silica membranes for gas separation, J. Membr. Sci. 143 (1998) 37.
[27] J.C. Diniz da Costa, G.Q. Lu, V. Rudolph, Y.S. Lin, Novel molecular sieve silica (MSS) membranes: characterisation and permeation of single-step and two-step sol–gel membranes, J. Membr. Sci. 198 (2002) 9.
[28] R.M. Barrer, Porous crystal membranes, J. Chem. Soc., Faraday Trans. 86 (1990) 1123.
[29] H.Y. Ha, S.W. Nam, S.A. Hong, W.K. Lee, Chemical vapor deposition of hydrogen permselective silica films on porous–glass supports from tetraethylorthosilicate, J. Membr. Sci. 85 (1993) 279.
[30] S. Nakao, T. Suzuki, T. Sugawara, T. Tsuru, S. Kimura, Preparation of microporous membranes by TEOS/O-3 CVD in the opposing reactants geometry, Micropor. Mesopor. Mater. 37 (2000) 145.
[31] S. Gopalakrishnan, Y. Yoshino, M. Nomura, B.N. Nair, S.I. Nakao, A hybrid processing method for high performance hydrogen-selective silica membranes, J. Membr. Sci. 297 (2007) 5.
[32] D.W. Breck, Zeolite Molecular Sieves––Structure, Chemistry, and Use, John Wiley & Sons, New York, 1974, p. 636.
[33] T.C. Bowen, H. Kalipcilar, J.L. Falconer, R.D. Noble, Pervaporation of organic/water mixtures through B-ZSM-5 zeolite membranes on monolith supports, J. Membr. Sci. 215 (1–2) (2003) 235.
[34] M.E. van Leeuwen, Derivation of stockmayer potential parameters for polar fluids, Fluid Phase Equilibr. 99 (1994) 1.
[35] G.J. Young, Interaction of water vapor with silica surfaces, J. Colloid Sci. 13 (1958) 67.